Supporting Information

Interface Engineering of Oxygen-Vacancy-Rich $NiCo_2O_4$/NiCoP Heterostructure as an Efficient Bifunctional Electrocatalyst for Overall Water-Splitting

Wei Jin, Jianping Chen, Hengbo Wu, Nan Zang, Qingwei Li, Weiquan Cai,* ZexingWu,*

Prof. Z. Wu

State Key Laboratory Base of Eco-chemical Engineering, College of Chemistry and Molecular Engineering, Qingdao University of Science & Technology, 53 Zhengzhou Road, 266042, Qingdao, P. R. China

Prof. W. Jin, J. Chen, H. Wu, and N. Zang

School of Chemical and Material Engineering, Jiangnan University, Wuxi 214122, China.

Dr. W. Cai

School of Chemistry and Chemical Engineering, Guangzhou University, 230 Guangzhou University City Outer Ring Road, Guangzhou 510006, China.

Prof. Q. Li

Advanced Research Institute for Multidisciplinary Science, Qilu University of Technology (Shandong Academy of Sciences), Jinan 250353, Shandong Province, P. R. China

*E-mail: cccaiwq@gzhu.edu.cn (W. Cai); splswzx@qust.edu.cn (Z. Wu)

Part I: Materials and Methods

Reagents and materials

Analytical-grade cobaltous nitrate hexahydrate ($Co(NO_3)_2 \cdot 6H_2O$), Nickel(II) nitrate hexahydrate ($Ni(NO_3)_2 \cdot 6H_2O$), urea (CH_4N_2O), anhydrous ethanol (EtOH), sodium hypophosphite ($NaH_2PO_2 \cdot H_2O$) and potassium hydroxide (KOH) were purchased from Sinopharm Chemical Reagent Co., Ltd. Commercial Pt/C and IrO_2 were purchased from Macklin and Aladdin, respectively. 5 wt.% Nafion was purchased from Aladdin and Alfa Aesar, respectively. All reagents and chemicals were used without further purification.

Synthesis of $NiCo_2O_4$/NiCoP heterostructure

Typically, 1 mmol $Ni(NO_3)_2 \cdot 6H_2O$ and 2 mmol $Co(NO_3)_2 \cdot 6H_2O$ were firstly added into 15 mL mixed solution of deionized water and ethanol (V_{H_2O} : V_{EtOH} = 3 : 0, 2 : 1, 1 : 1, 1 : 2, 0 : 3, respectively) in stirring for 60 min to form a uniform solution. Then, 10 mmol urea was added into the above dispersion and further stirred for another 60 min. The obtained solution was transferred into 25 mL autoclave with a Teflon liner at 160 ^oC, and kept for 12 h. The obtained product was centrifugal, and then washed with distilled water for several times, and dried at 60 °C in vacuum. The above samples were recorded as NiCo precursors-1/2/3/4/5, respectively.

Afterwards, NiCo precursors and 1 g $NaH_2PO_2 \cdot H_2O$ were placed in the central and upstream positions of a tube furnace, respectively. After flushed with Ar, the center of the tube furnace was elevated to 300 °C at a ramping rate of 2 °C min^{-1} and held at this temperature for 30 min, and then naturally cooled to ambient temperature under Ar to yield the $NiCo_2O_4$/NiCoP heterostructure.

For comparison, NiCoP was prepared under the similar experimental conditions, but with 1.5 $NaH_2PO_2 \cdot H_2O$ in the phosphidation process. The $NiCo_2O_4$ was also obtained via a similar experimental process, but without any $NaH_2PO_2 \cdot H_2O$ in phosphidation process.

Physicochemical characterization

The surface morphology was measured by field-emission scanning electron microscopy (FE-SEM, JSM-7610F). High resolution transmission electron

microscopy (HR-TEM) was determined by a JEOL JEM-2100F microscope. The crystalline phase was identified by XRD (X'Pert Pro MPD, Panalytical Company, Cu-Kα X-ray source). X-ray photoelectron spectroscopy (XPS) was identified on a VG ESCALAB MKII spectrometer with an Mg Ka X-ray source. The electron spin resonance (ESR) analysis was obtained on a JEOL spectrometer (JES-FA200) at ambient temperature.

Electrochemical Measurements

Electrochemical measurements were carried out with a CHI 760E electrochemical analyzer. A standard three-electrode system was used, including a rotating disk electrode (RDE) as the working electrodes (0.196 cm^2), a carbon rod as the auxiliary electrode, and a Ag/AgCl as the reference electrode. The catalyst ink was prepared by ultrasonically dispersing the mixture of 5 mg of catalyst, 0.5 mL ethanol, 0.5 mL deionized water and 20 μL of 5 wt.% Nafion solution. 10 μL of the catalyst ink was pipetted and spread onto the electrode. The loading of the studied catalysts was 250 μg cm^{-2}.

For the OER, the polarization curves were measured in 1 M KOH solution recorded from 1.1 to 2.0 V at a scan rate of 5 mV s^{-1}. Note that high-purity O_2 was bubbled through the electrolyte during the testing to fix the reversible oxygen potential (or ensure the O_2/H_2O equilibrium at 1.23 V *vs.* RHE). To avoid the peeling of catalyst caused by evolved O_2 adhesion, a rotation speed of 1600 rpm was offered during the OER. For the HER test, the measurements were also carried out in 1 M KOH solution with a scan rate of 5 mV s^{-1} and 1600 rpm rotating speeds. Before testing, N_2 was passed through the electrolyte for at least 20 min to saturate the electrolyte with N_2. The impedance was tested by electrochemical impedance spectroscopy measurements in a frequency range from 0.1 Hz to 100 kHz at open circuit potential with 5 mV amplitude of sinusoidal potential perturbation.

The overall water splitting was tested in the two-electrode scheme in 1 M KOH. The $NiCo_2O_4$/NiCoP was dropped onto a carbon paper substrate in both the anode and cathode. The catalyst loading is 0.6 mg cm^{-2}.

Part II: Figures and Tables

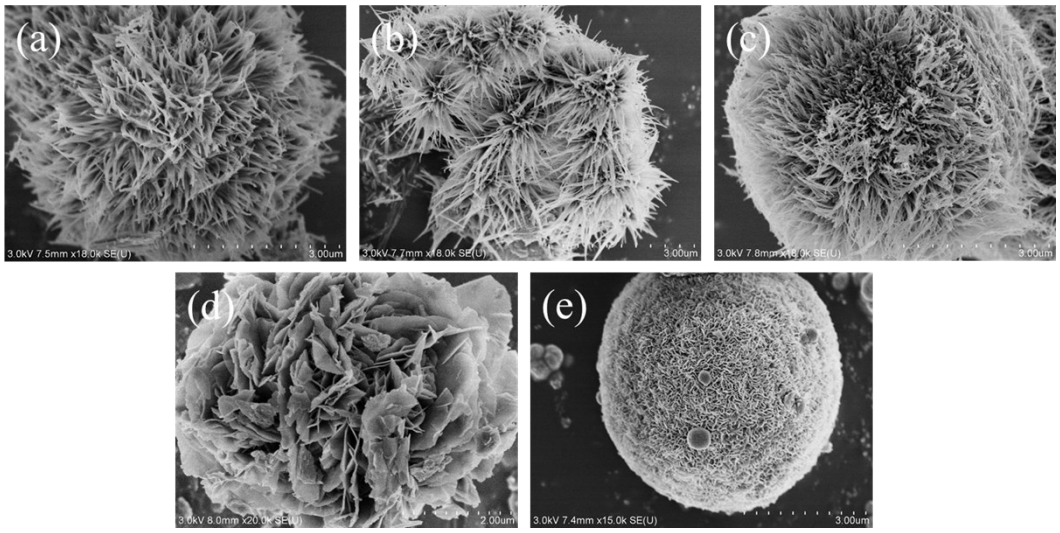

Figure S1. SEM images of (a) NiCo precursor-1, (b) NiCo precursor-2, (c) NiCo precursor-3, (d) NiCo precursor-4 and (e) NiCo precursor-5.

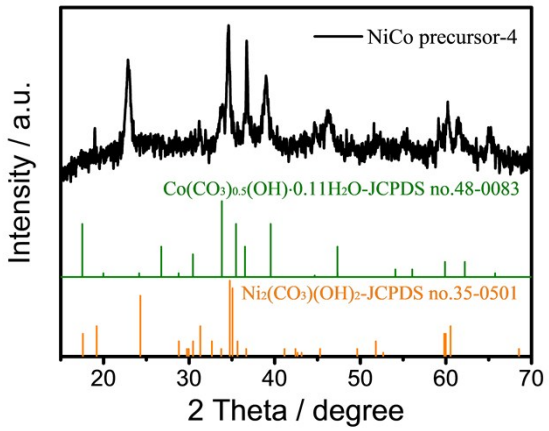

Figure S2. XRD pattern of NiCo precursor-4.

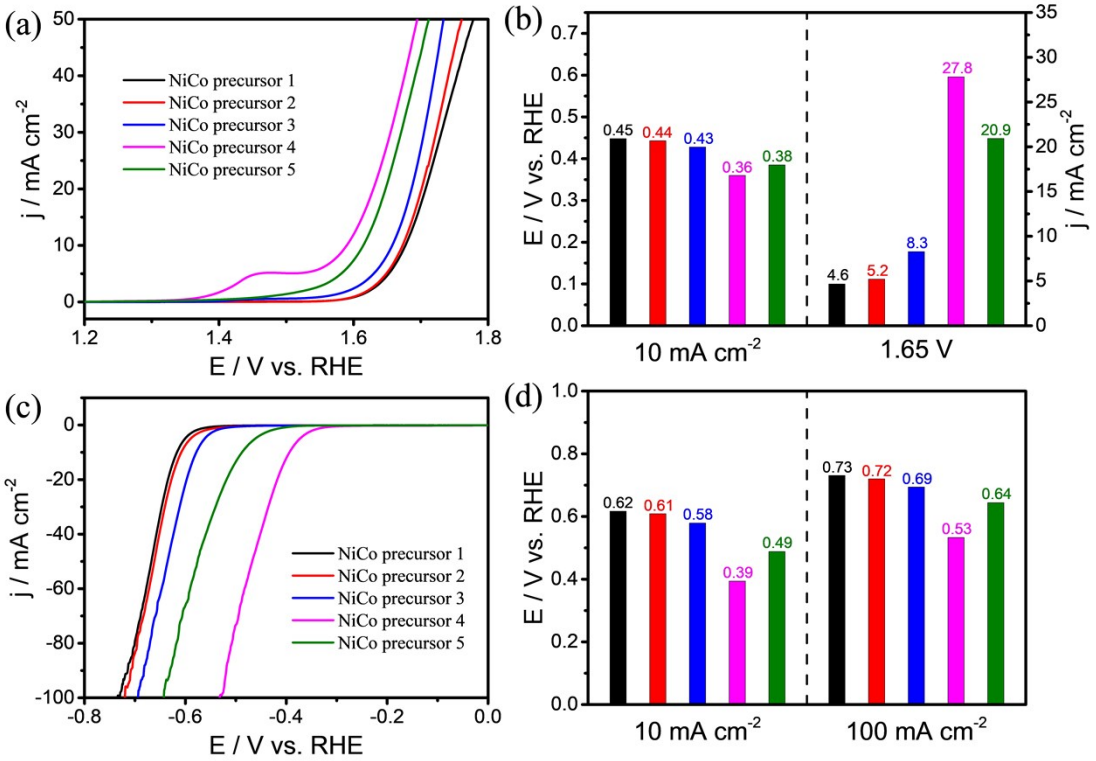

Figure S3. (a) OER polarization curves in O_2-saturated 1 M KOH of NiCo precursors; (b) Overpotentials at a chosen current density of 10 mA cm^{-1} and the current densities at a chosen potential of 1.65 V; (c) HER polarization curves in N_2-saturated 1 M KOH of NiCo precursors; (d) Potentials at a chosen current density of 10 and 100 mA cm^{-1}.

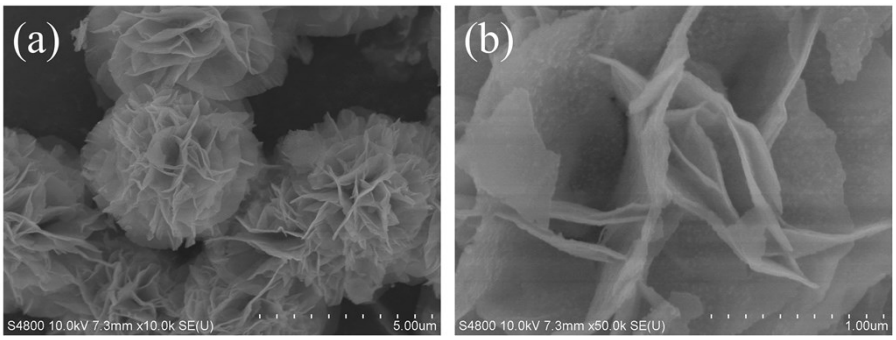

Figure S4. (a and b) SEM images of $NiCo_2O_4$/NiCoP at different magnification.

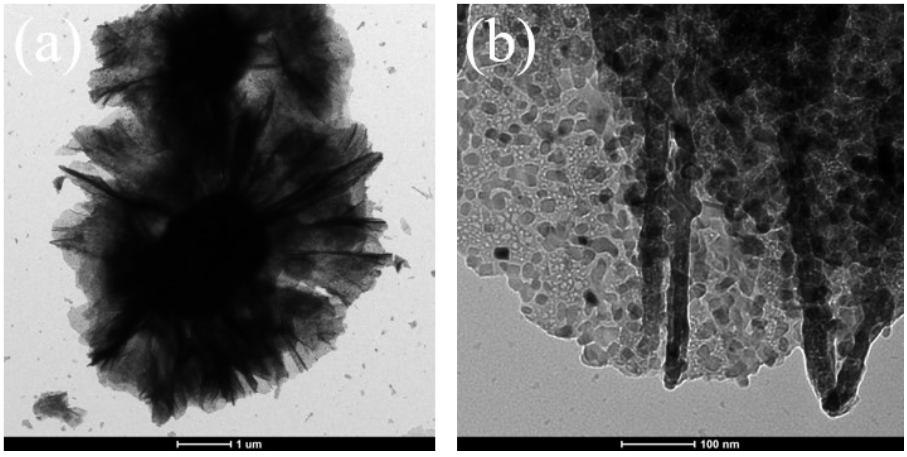

Figure S5. (a and b) TEM images of $NiCo_2O_4$/NiCoP at different magnification.

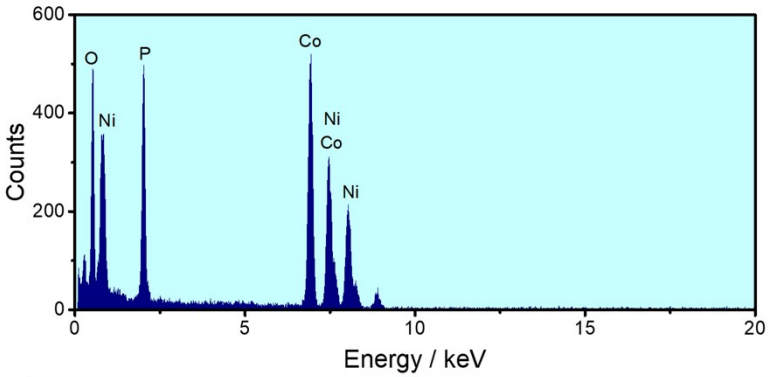

Element	Atomic %
Ni(K)	13.56
Co(K)	19.94
O(K)	50.01
P(K)	16.47

Figure S6. EDX spectrum of $NiCo_2O_4$/NiCoP and atom percentage of Ni, Co, O and P.

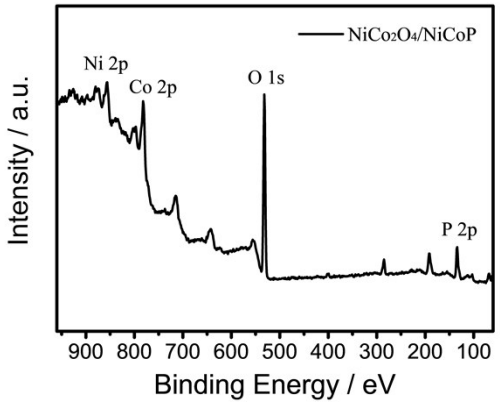

Figure S7. Full XPS spectrum of $NiCo_2O_4$/NiCoP.

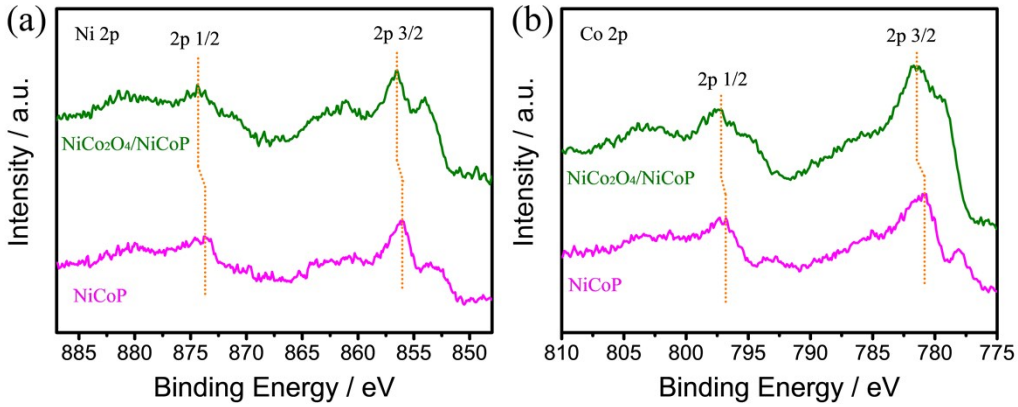

Figure S8. XPS spectra of (a) Ni 2p, (b) Co 2p in $NiCo_2O_4$/NiCoP and NiCoP.

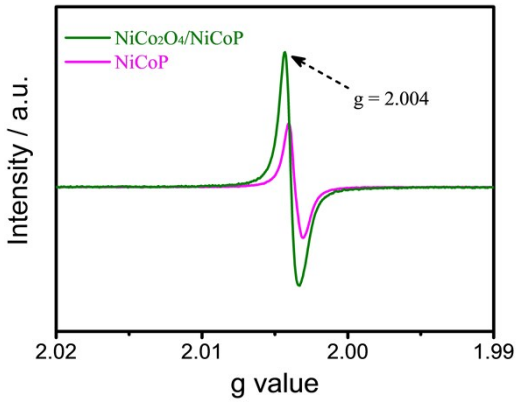

Figure S9. ESR spectra of $NiCo_2O_4$/NiCoP and NiCoP.

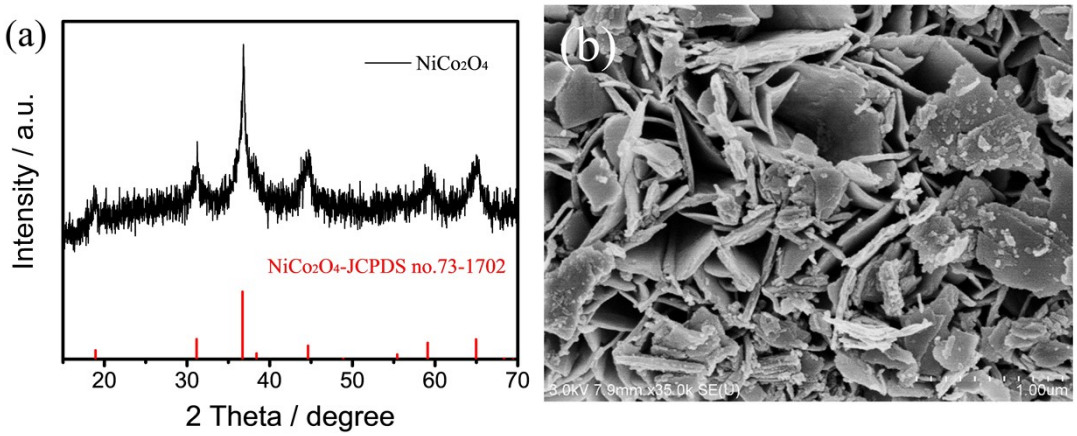

Figure S10. (a) XRD pattern and (b) SEM image of $NiCo_2O_4$.

The $NiCo_2O_4$ composite was prepared by the similar procedure with $NiCo_2O_4$/NiCoP except the exclusion of $NaH_2PO_2 \cdot H_2O$ in phosphidation process. The $NiCo_2O_4$ composite shows the distinct characteristic peaks correspond to $NiCo_2O_4$ (JCPDS Card No. 73-1702), confirming the formation of $NiCo_2O_4$. In addition, SEM images show that $NiCo_2O_4$ displayed a disordered sheet structure.

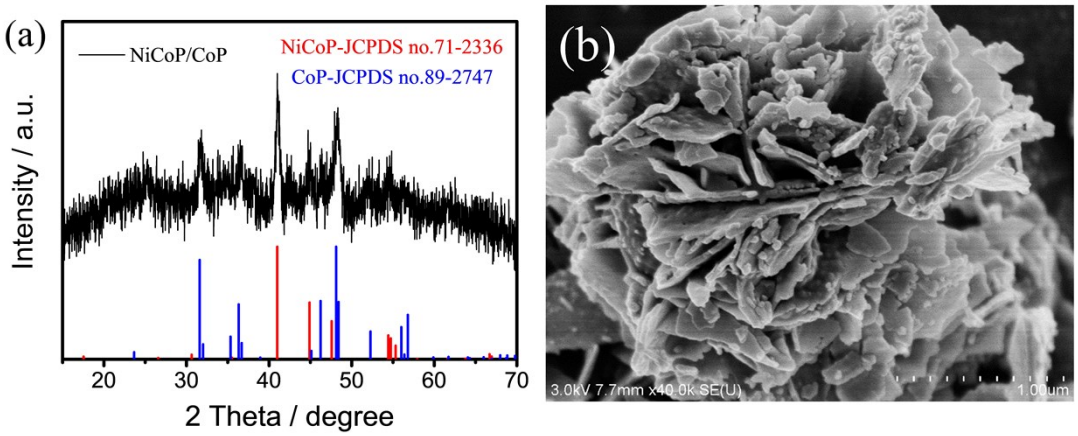

Figure S11. (a) XRD pattern and (b) SEM image of NiCoP.

The NiCoP composite was prepared by the similar procedure with $NiCo_2O_4$/NiCoP except the addition of 1.5 $NaH_2PO_2 \cdot H_2O$ in the phosphidation process. The NiCoP composite shows the distinct characteristic peaks correspond to NiCoP (JCPDS Card No. 71-2336) and CoP (JCPDS Card No. 89-2747), respectively, indicating the successful fabrication of NiCoP. Besides, SEM images show that NiCoP displayed the irregular porous nanosheets.

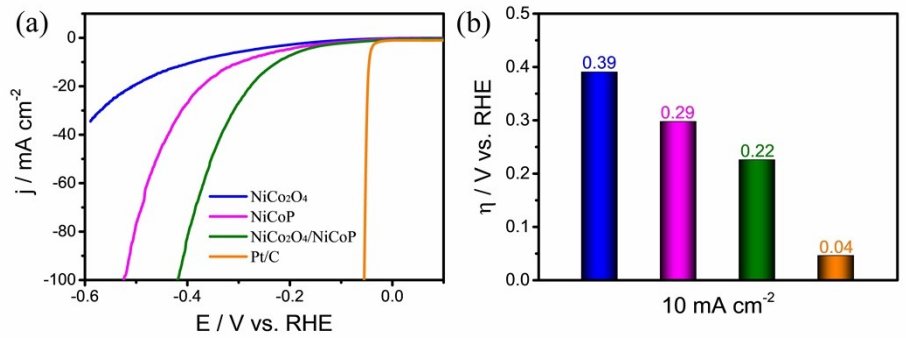

Figure S12. (a) HER polarization curves in N_2-saturated 0.5 M H_2SO_4 of $NiCo_2O_4$, NiCoP, $NiCo_2O_4$/NiCoP and commercial Pt/C catalysts. (b) Overpotentials at chosen current density of 10 mA cm^{-2}.

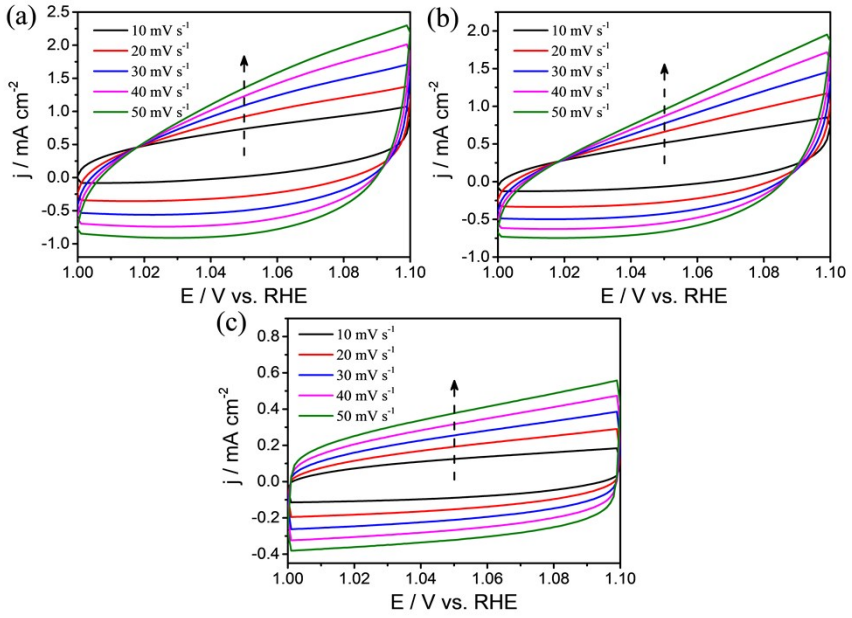

Figure S13. Cyclic voltammograms curves at different scan rates of (a) $NiCo_2O_4$/NiCoP, (b) NiCoP and (c) $NiCo_2O_4$.

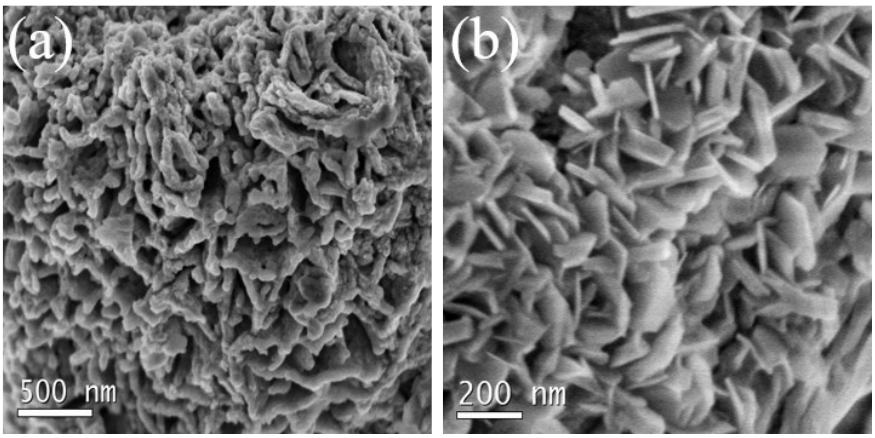

Figure S14. (a and b) SEM images of $NiCo_2O_4$/NiCoP after durability test of 12 h.

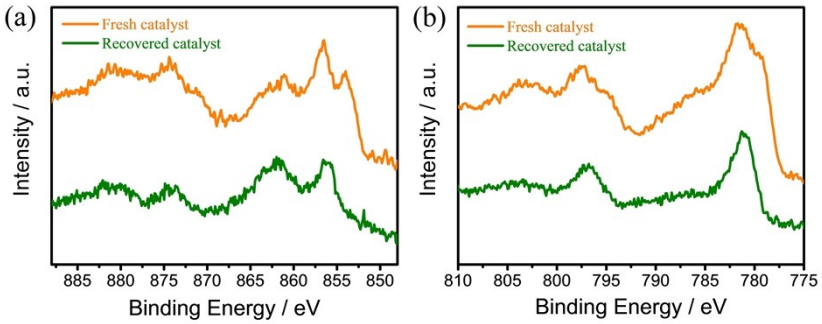

Figure S15. High-resolution XPS spectra of NiCo2O4/NiCoP after durability test at (a) Ni 2p and (b) Co 2p region.

Table S1. Performances of recently reported OER electrocatalysts. Herein, the comparison of OER activity of $NiCo_2O_4$/NiCoP with previously reported cobalt based materials and other non-noble metal electrocatalysts were made.

Catalyst	Overpotential / mV (10 mA cm^{-2})	Electrolyte	Loadings (mg cm^{-2})	Ref
$NiCo_2O_4$/NiCoP	295	1 M KOH	0.25	This work
$Ni_{0.6}Co_{1.4}P$	300	1 M KOH	0.35	[1]
CoNi LDH/CoO	300	1 M KOH	0.265	[2]
CoOx	306	1 M KOH	0.5	[3]
$NiCo_2O_4$ nanosheets	320	1 M KOH	0.28	[4]
CoMn LDH	324	1 M KOH	0.142	[5]
CoO nanorods	330	1 M KOH	0.19	[6]
$Co_3O_4/NiCo_2O_4$	340	1 M KOH	1	[7]
Reduced Co_3O_4 nanowire	380	1 M KOH	0.136	[8]
Co_3O_4@CoO	430	1 M KOH	0.077	[9]

Table S2. Comparison of HER activity of $NiCo_2O_4$/NiCoP with other HER catalysts reported before.

Catalyst	Overpotential / mV (10 mA cm^{-2})	Electrolyte	Loadings (mg cm^{-2})	Ref
$NiCo_2O_4$/NiCoP	198	1 M KOH	0.25	This work
$Co_{0.6}Mo_{1.4}N_2$	200	0.1 M $HClO_4$	0.243	[10]
CoP/CC	209	1 M KOH	0.92	[11]
NiCoP/rGO	209	1 M KOH	N/A	[12]
CoP@BCN	215	1 M KOH	0.4	[13]
$Cu_{0.3}Co_{2.7}P$/NC	220	1 M KOH	N/A	[14]
CoP/RGO-0.36	250	0.5 M H_2SO_4	0.29	[15]
$Co_{0.32}Ni_{0.68}S_2$ film	276	0.5 M H_2SO_4	N/A	[16]
CoS_2/rGO	278	0.5 M H_2SO_4	0.28	[17]
Co-NRCNTs	370	1 M KOH	0.28	[18]

Table S3. Comparison of the overall water splitting activity of NiCo2O4/NiCoP with those of the previously reported non-noble metal catalysts.

Catalyst	Voltage / V (10 mA cm^{-2})	Electrolyte	Ref
$NiCo_2O_4$/NiCoP	1.66	1 M KOH	This work
$CoNi(OH)_x$ || NiN_x	1.67	1 M KOH	19
NiFe/$NiCo_2O_4$	1.67	1 M KOH	20
$NiCo_2S_4$	1.68	1 M KOH	21
Co_1Mn_1CH	1.68	1 M KOH	22
CoP/rGO	1.7	1 M KOH	23
CoO/MoO_x	1.72	1 M KOH	24
$NiCo_2O_4$ || $Ni_{0.33}Co_{0.67}S_2$ NWs	1.73	1 M KOH	25
CP/CTs/Co-S	1.74	1 M KOH	26
$NixCo_{3-X}O_4$ || $NiCo/NiCoO_x$	1.75	1 M KOH	27

Part III: References

(1) Qiu, B.; Cai, L.; Wang, Y.; Lin, Z.; Zuo, Y.; Wang, M.; Chai, Y. Fabrication of Nickel-Cobalt Bimetal Phosphide Nanocages for Enhanced Oxygen Evolution Catalysis. *Adv. Funct. Mater.* **2018**, *28*, 1706008.

(2) Wu, J.; Ren, Z.; Du, S.; Kong, L.; Liu, B.; Xi, W.; Zhu, J.; Fu, H. A highly active oxygen evolution electrocatalyst: Ultrathin CoNi double hydroxide/CoO nanosheets synthesized via interface-directed assembly. *Nano Res.* **2016**, *9*, 713-725.

(3) Xu, W.; Lyu, F.; Bai, Y.; Gao, A.; Feng, J.; Cai, Z.; Yin, Y. Porous cobalt oxide nanoplates enriched with oxygen vacancies for oxygen evolution reaction. *Nano Energy* **2018**, *43*, 110-116.

(4) Bao, J.; Zhang, X.; Fan, B.; Zhang, J.; Zhou, M.; Yang, W.; Hu, X.; Wang, H.; Pan, B.; Xie, Y. Ultrathin Spinel-Structured Nanosheets Rich in Oxygen Deficiencies for Enhanced Electrocatalytic Water Oxidation. *Angew. Chem.* **2015**, *127*, 7501-7512.

(5) Song, F.; Hu, X. Ultrathin cobalt-manganese layered double hydroxide is an efficient oxygen evolution catalyst. *J. Am. Chem. Soc.* **2014**, *136*, 16481-16484.

(6) Ling, T.; Yan, D. Y.; Jiao, Y.; Wang, H.; Zheng, Y.; Zheng, X.; Mao, J.; Du, X. W.; Hu, Z.; Jaroniec, M.; Qiao, S. Z. Engineering surface atomic structure of single-crystal cobalt (II) oxide nanorods for superior electrocatalysis. *Nat. Commun.* **2016**, *7*, 12876.

(7) Hu, H.; Guan, B.; Xia, B.; Lou, X. W. Designed Formation of Co_3O_4/$NiCo_2O_4$ Double-Shelled Nanocages with Enhanced Pseudocapacitive and Electrocatalytic Properties. *J. Am. Chem. Soc.* **2015**, *137*, 5590-5595.

(8) Wang, Y.; Zhou, T.; Jiang, K.; Da, P.; Peng, Z.; Tang, J.; Kong, B.; Cai, W.-B.; Yang, Z.; Zheng, G. Reduced Mesoporous Co_3O_4 Nanowires as Efficient Water Oxidation Electrocatalysts and Supercapacitor Electrodes. *Adv. Energy Mater.* **2014**, *4*, 1400696.

(9) Bergmann, A.; Martinez-Moreno, E.; Teschner, D.; Chernev, P.; Gliech, M.; de Araujo, J. F.; Reier, T.; Dau, H.; Strasser, P. Reversible amorphization and the catalytically active state of crystalline Co_3O_4 during oxygen evolution. *Nat. Commun.*

2015, *6*, 8625.

(10) Cao, B.; Veith, G. M.; Neuefeind, J. C.; Adzic, R. R.; Khalifah, P. G. Mixed close-packed cobalt molybdenum nitrides as non-noble metal electrocatalysts for the hydrogen evolution reaction. *J. Am. Chem. Soc.* **2013**, *135*, 19186-19192.

(11) Tian, J.; Liu, Q.; Asiri, A. M.; Sun, X. Self-supported nanoporous cobalt phosphide nanowire arrays: an efficient 3D hydrogen-evolving cathode over the wide range of pH 0-14. *J. Am. Chem. Soc.* **2014**, *136*, 7587-7590.

(12) Li, J.; Yan, M.; Zhou, X.; Huang, Z.-Q.; Xia, Z.; Chang, C.-R.; Ma, Y.; Qu, Y. Mechanistic Insights on Ternary $Ni_{2-X}Co_XP$ for Hydrogen Evolution and Their Hybrids with Graphene as Highly Efficient and Robust Catalysts for Overall Water Splitting. *Adv. Funct. Mater.* **2016**, *26*, 6785-6796.

(13) Tabassum, H.; Guo, W.; Meng, W.; Mahmood, A.; Zhao, R.; Wang, Q.; Zou, R. Metal-Organic Frameworks Derived Cobalt Phosphide Architecture Encapsulated into B/N Co-Doped Graphene Nanotubes for All pH Value Electrochemical Hydrogen Evolution. *Adv. Energy Mater.* **2017**, *7*, 1601671.

(14) Song, J.; Zhu, C.; Xu, B. Z.; Fu, S.; Engelhard, M. H.; Ye, R.; Du, D.; Beckman, S. P.; Lin, Y. Bimetallic Cobalt-Based Phosphide Zeolitic Imidazolate Framework: CoPx Phase-Dependent Electrical Conductivity and Hydrogen Atom Adsorption Energy for Efficient Overall Water Splitting. *Adv. Energy Mater.* **2017**, *7*, 1601555.

(15) Ma, L.; Shen, X.; Zhou, H.; Zhu, G.; Ji, Z.; Chen, K. CoP nanoparticles deposited on reduced graphene oxide sheets as an active electrocatalyst for the hydrogen evolution reaction. *J. Mater. Chem. A* **2015**, *3*, 5337-5343.

(16) Kong, D.; Cha, J. J.; Wang, H.; Lee, H. R.; Cui, Y. First-row transition metal dichalcogenide catalysts for hydrogen evolution reaction. *Energ. Environ. Sci.* **2013**, *6*, 3553.

(17) Peng, S.; Li, L.; Han, X.; Sun, W.; Srinivasan, M.; Mhaisalkar, S. G.; Cheng, F.; Yan, Q.; Chen, J.; Ramakrishna, S. Cobalt sulfide nanosheet/graphene/carbon nanotube nanocomposites as flexible electrodes for hydrogen evolution. *Angew. Chem.* **2014**, *126*, 12802 -12807.

(18) Zou, X.; Huang, X.; Goswami, A.; Silva, R.; Sathe, B. R.; Mikmekova, E.; Asefa,

T. Cobalt-embedded nitrogen-rich carbon nanotubes efficiently catalyze hydrogen evolution reaction at all pH values. *Angew. Chem. Int. Ed.* **2014**, *53*, 4372-4376.

(19) You, B.; Sun, Y. Hierarchically Porous Nickel Sulfide Multifunctional Superstructures. *Adv. Energy Mater.* **2016**, *6*, 1502333.

(20) Xiao, C.; Li, Y.; Lu, X.; Zhao, C. Bifunctional Porous NiFe/$NiCo_2O_4$/Ni Foam Electrodes with Triple Hierarchy and Double Synergies for Efficient Whole Cell Water Splitting. *Adv. Funct. Mater.* **2016**, *26*, 3515-3523.

(21) Liu, D.; Lu, Q.; Luo, Y.; Sun, X.; Asiri, A. M. $NiCo_2S_4$ nanowires array as an efficient bifunctional electrocatalyst for full water splitting with superior activity. *Nanoscale* **2015**, *7*, 15122-15126.

(22) Tang, T.; Jiang, W. J.; Niu, S.; Liu, N.; Luo, H.; Chen, Y. Y.; Jin, S. F.; Gao, F.; Wan, L. J.; Hu, J. S. Electronic and Morphological Dual Modulation of Cobalt Carbonate Hydroxides by Mn Doping toward Highly Efficient and Stable Bifunctional Electrocatalysts for Overall Water Splitting. *J. Am. Chem. Soc.* **2017**, *139*, 8320-8328.

(23) Jiao, L.; Zhou, Y. X.; Jiang, H. L. Metal-organic framework-based CoP/reduced graphene oxide: high-performance bifunctional electrocatalyst for overall water splitting. *Chem. Sci.* **2016**, *7*, 1690-1695.

(24) Yan, X.; Tian, L.; Atkins, S.; Liu, Y.; Murowchick, J.; Chen, X. Converting $CoMoO_4$ into CoO/MoOx for Overall Water Splitting by Hydrogenation. *ACS Sustain. Chem. Eng.* **2016**, *4*, 3743-3749.

(25) Peng, Z.; Jia, D.; Al-Enizi, A. M.; Elzatahry, A. A.; Zheng, G. From Water Oxidation to Reduction: Homologous Ni-Co Based Nanowires as Complementary Water Splitting Electrocatalysts. *Adv. Energy Mater.* **2015**, *5*, 1402031.

(26) Wang, J.; Zhong, H. X.; Wang, Z. L.; Meng, F. L.; Zhang, X. B. Integrated Three-Dimensional Carbon Paper/Carbon Tubes/Cobalt-Sulfide Sheets as an Efficient Electrode for Overall Water Splitting. *ACS nano* **2016**, *10*, 2342-2348.

(27) Pu, Z.; Luo, Y.; Asiri, A. M.; Sun, X. Efficient Electrochemical Water Splitting Catalyzed by Electrodeposited Nickel Diselenide Nanoparticles Based Film. *ACS Appl. Mater. Interfaces* **2016**, *8*, 4718-4723.